INTERNATIONAL JOURNAL OF INTEGRATED ENGINEERING
ISSN: 2229-838X e-ISSN: 2600-7916

IJIE

Vol. 17 No. 4 (2025) 288-300
https://publisher.uthm.edu.my/ojs/index.php/ijie

A Novel Study of Orifice Dimension and Hemodynamic Parameter Changes in Healthy and Stenotic Aortic Valve During Peak Systole

Nur'Afifah Yousri[1], Nabilah Ibrahim[1]*, Muhammad Riddha Abdul Rahman[2], Ali Kamil Kareem[3]

[1] *Department of Electronics Engineering, Universiti Tun Hussein Onn Malaysia, 86400, Batu Pahat, Johor, MALAYSIA*
[2] *Faculty of Health Sciences, Universiti Sultan Zainal Abidin (UnisZA), 21300, Terengganu, MALAYSIA*
[3] *Biomedical Engineering Department, Al-Mustaqbal University College, Babylon, IRAQ*

*Corresponding Author: nabilah@uthm.edu.my
DOI: https://doi.org/10.30880/ijie.2025.17.04.025

Article Info

Received: 10 April 2025
Accepted: 13 October 2025
Available online: 25 November 2025

Keywords

Aortic valve, computational method, blood velocity, blood pressure, peak flow, TAWSS, RRT, OSI

Abstract

This study examined the hemodynamics characteristic of normal and stenotic aortic valves through computational fluid dynamics (CFD) simulations using ANSYS software. Two models were developed, a fully opened healthy valve (100% orifice) and a partially opened stenotic valve (50% orifice) that evaluated at peak systolic flow. The aim was to visualize blood flow patterns on the velocity, pressure, and statistical parameters including kurtosis, mean, standard deviation, and skewness along the aortic vessel near the valve region. Results show that the stenotic model exhibited a significant increase in peak velocity, reaching 6.09 m/s, compared to 1.50 m/s in the healthy model. It consistent with clinically observed values in severe aortic stenosis. A notable pressure drop was also observed across the stenotic valve that indicating increased flow resistance. This finding highlights how stenosis severity alters local hemodynamics and are relevant for identifying regions at risk of vascular damage. This study contributes to improved diagnostic strategies for aortic stenosis by linking valve orifice size to key hemodynamic risk indicators such as time-average wall shear stress (TAWSS), oscillatory shear index (OSI), and relative residence time (RRT).

1. Introduction

Aortic valve stenosis (AS) is a prevalent and clinically significant valvular heart disease characterized by the narrowing of the aortic valve opening, leading to left ventricular outflow obstruction and decreased cardiac performance, thereby affecting blood circulation from the heart to the body [1]. The condition is projected to impact a significant portion of seniors, with a prevalence of roughly 5% among those aged 65, and this figure rises dramatically with increasing age [1]-[4]. AS is associated with a high mortality rate, particularly if left untreated, and can lead to symptoms such as chest pain, heart failure, and syncope [5]. Given AS's progressive nature and significant impact on patient outcomes, developing innovative diagnostic and treatment strategies is crucial to address this condition effectively. The definitive treatment for severe aortic stenosis (AS) is aortic valve replacement (AVR). Recent research has indicated a growing interest in utilizing transcatheter aortic valve

replacement (TAVR) for patients with less than severe AS and exploring medical therapies to reduce or prevent disease progression [4].

While velocity analysis is an essential tool in understanding the hemodynamic of the aortic valve, particularly during systole, and its potential to provide valuable insights into the progression and management of AS, current diagnostic methods have limitations. For instance, echocardiographic assessment of AS relies on clinical parameters such as peak velocity, mean pressure gradient, and aortic valve area (AVA) to determine the hemodynamic impact of the effective orifice area and assess the severity of AS [2],[6],[7]. However, echocardiographic parameters for assessing AS severity overlook the "pressure recovery" phenomenon, in which velocity analysis offers a more precise evaluation [6],[7]. Moreover, the severity of AS is not solely based on valve hemodynamic but also underlying left ventricular dysfunction and comorbidities, necessitating a shift from "standardization" to "individualization" in diagnosis and prognostication [1].

Computational tools like Computational Fluid Dynamics (CFD) offer a powerful solution by enabling detailed, patient-specific analysis of valve flow dynamics. CFD simulation software can provide a detailed and accurate analysis of blood flow patterns in the aortic valve, which could help better understand the pathophysiology of AS and develop personalized treatment strategies [8]. By providing valuable insights into the hemodynamic of the aortic valve, velocity analysis can contribute to the development of innovative diagnostic and treatment methods for AS [6]-[8]. Using CFD simulation software to study blood flow in the aortic valve offers key benefits for improving diagnostics, treatment planning, and managing aortic valve diseases. CFD provides detailed hemodynamic insights, enabling analysis of complex pressure and flow patterns, including metrics like wall shear stress (WSS) and pressure differences [9],[10]. When combined with cardiovascular imaging, CFD supports personalized medicine by estimating patient-specific hemodynamic outcomes before interventions as part of precision medicine [10],[11]. Furthermore, CFD findings correlate with clinical outcomes, especially in aortic valve replacement and hemodynamic changes, aiding in validation and prediction [10],[12],[13]. Despite hurdles such as extended execution periods, high computational costs, and the necessity for multidisciplinary knowledge, progress is being made to overcome these obstacles, encouraging broader clinical adoption of CFD technology.

Artificial intelligence and computational methods are also being explored to identify AS in asymptomatic patients [1]. However, while several recent studies have made valuable contributions to understanding the hemodynamic of aortic valve stenosis, many have focused on flow visualization and pressure gradient without quantifying statistical parameters such as kurtosis, mean, standard deviation, and skewness. For example, the study by Zolfaghari et al. [14] investigated wall shear stress and pressure patterns of aortic valve stenosis but did not present other statistical parameters. This highlights a significant gap in current research where statistical parameters could offer deeper insights into abnormal blood flow characteristics in the aortic valve. Thus, this study aims to visualize the blood flow characteristics due to variations in aortic valve geometry generated from computational simulations. Additionally, the simulation will employ various sizes of valve orifices of simplified models for both healthy and stenotic conditions, utilizing different inlet velocities. Critical parameters are also to be investigated by evaluating the hemodynamic effects of various aortic valve configurations. This study applies boundary conditions at the aortic valve model, which are inlet, wall (rigid), and outlet, focused on the systole phase. At this point, the flow is assumed to be turbulent based on the Reynolds number above 5000. By assuming rigid walls and simplified conditions of aortic valve models, this study allows for a focused investigation into how the size and thickness of the valve orifice affect flow behavior during the systole phase.

2. Method

2.1 Method Workflow

This study aimed to analyse blood flow patterns within the aortic valve using CFD simulation software. The following workflow shown in Fig. 1, is considered. Firstly, a schematic diagram of the aortic valve was created before the data geometry at the aortic vessel was collected. This initial step is crucial to accurately measuring the length and dimension of the aortic valve structure before designing it using CAD software [15]. Secondly, based on the schematic diagram, CAD software is employed to create both healthy and stenotic models. This step ensures the details and precision of models are for accurate simulation. Thirdly, the discretisation technique was applied to set up the models in the CFD software. The meshing process was initiated to solve the governing equations, i.e., the Navier Stokes equations. After discretisation, the inlet velocity profile for the aortic valve model was established at peak flow (PF). In this setup, the inlet velocity was established to examine the behaviour of blood as it flows through the valve, ultimately facilitating a thorough analysis of hemodynamic parameters. Next, the model properties and boundary conditions were defined. This study emphasises the properties of the model concerning the aortic valve and the aortic root (blood vessel). In the meantime, three boundaries were established for the boundary condition: the inlet, the wall, and the outlet. Parameter assumptions were defined at this stage, such as the blood flow, which was set up as incompressible fluid. Meanwhile, the density of blood and viscosity are set constant as 1060 kg/m^3 and 0.0035 Pa.s, respectively.

Int. Journal of Integrated Engineering Vol. 17 No. 4 (2025) p. 288-300

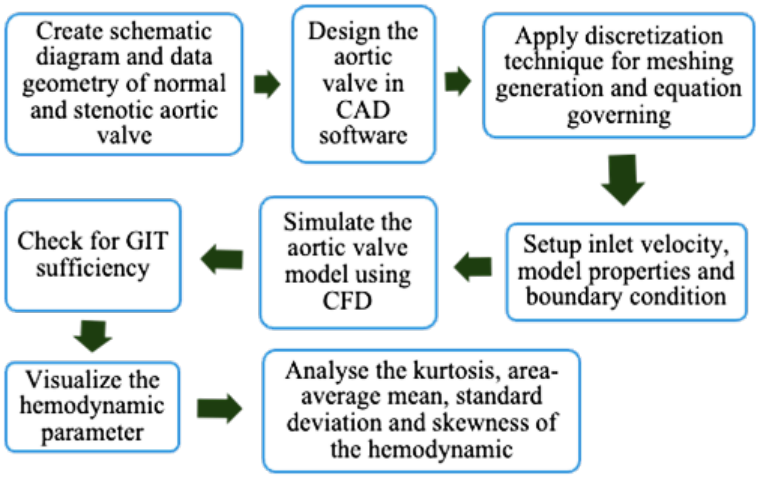

Fig. 1 *Workflow of the study using simplified models of a healthy valve (100% orifice) and a stenotic valve (50% orifice) with varying orifice and thickness of the valve to visualise the velocity, pressure followed by analysis of statistical parameters of blood flow in the aortic valve*

2.2 Discretization Technique

Meshing for the geometry was done using tetrahedral patch-conforming method. A grid independence test (GIT) simulation was carried out to ensure the mesh quality appropriately reflects the flow behaviour [35], [16]. Nine mesh sizes have been conducted to ensure that the consistency of the results. If the grid is not sufficiently refined, the data would vary with the grid size [17]-[19]. In that case, the simulation must be run again at a meshing process in the discretization technique until the data error between GIT reaches a zero value. The number of element size was done ranging from 3.50 mm to 0.75 mm. the optimal mesh was selected at 0.80 mm where the GIT showed zero relative error between successive meshes. The final mesh consisted with a skewness value below 1 which is indicate a good mesh quality [20]. After completing the GIT, the study moves on to the final step in the processing stage: verifying data from the previous study. Data verification of the prior study is important to ensure the accuracy and reliability of the simulation result [21]. A steady-state solver was employed in this study because the simulation only focused on the Peak Flow phase. The k-ω SST turbulence model was used due to effectiveness in capturing near flow behavior. In case the result of the verification is contradictory, the simulation needs to be revised, including redesigning the aortic valve in CAD software.

Lastly, the post-processing was conducted using the Ansys software in the simulation. This stage is to analyse and interpret the simulation results. When the simulation results were verified, the healthy aortic valve and the stenotic aortic valve models across varying openings of the valve orifice would be visualised and analysed. The hemodynamic parameters include velocity, pressure, velocity streamline, time-average wall shear stress (TAWSS), oscillatory shear index (OSI), and relative residence time (RRT). The setup range of TAWSS, OSI, and RRT is shown in Table I. These parameters provide insights into the blood flow characteristics through the valve at different stages of the stenotic disease. In addition, the study assessed the aortic valve through statistical analyses, including kurtosis, area mean average, standard deviation, and skewness, to identify the risk model that differentiates between healthy and stenotic aortic valves. Moreover, the statistical analysis known as kurtosis, mean, standard deviation, and skewness were determined to predicted a risk at the vessel. Positive kurtosis indicates a heavy-tailed distribution which has more extreme data values, while negative kurtosis reflects a light tailed distribution that having a low kurtosis value [22].

Next, Skewness measures how symmetrical a dataset is [22]. A perfectly symmetrical distribution has equal shape on both sides of the center point. If the skewness is not zero, it means the distribution is asymmetrical [23], [24]. As skewness increases, kurtosis tends to increase as well. The mean represents the central value of data and is used to summarizes TAWSS, OSI and RRT [22]. Meanwhile, the standard deviation shows how spread out the data is by calculating the square root of the variance [22]. In the analysis of TAWSS, Kumar and Anurag [25] reported that an increase in kurtosis value reflects to the changes in flow patterns and highlights region of elevated shear stress which may contribute to turbulent flow condition and endothelial wall dysfunction. In the case of OSI, OSI play a role in the progression of aortic valve disease by impacting the structural integrity and functional performance of the valve [26]. Meanwhile, for the RRT, Barde et. al noted that greater dispersion in the data indicates higher variability whereas a lower standard deviation reflects reduced variability in the observed values [27].

Table 1 *Range of parameters*

Parameter	Range	Consequence
TAWSS	TAWSS ≥ 3.7 Pa	Trauma in blood vessel wall
OSI	OSI ≥ 0.2	Build a plaque
RRT	$3Pa^{-1} \leq RRT \leq 7Pa^{-1}$	Progression of the plaque

2.3 Inlet Velocity Setup, Parameter Assumption and Boundary Condition

2.3.1 Inlet Velocity Setup

As per the 2020 ACC/AHA guideline, severe aortic stenosis is characterised by an aortic peak velocity exceeding 4 m/s and a mean gradient surpassing 40 mmHg. This indicates that the blood flow velocity at the aortic root increases disproportionately to valve orifice size in patients with aortic stenosis. Fig. 2 illustrates the allocation of velocity profile in time duration that was set up in PlotDigitizer. Previously in [28], the reading was measured based on the echocardiography image in a pulsed Doppler mode. The cardiac was divided into six distinct phases [14]:

I. Middle acceleration (MA)
II. Three-quarters acceleration (3QA)
III. Peak flow (PF)
IV. Quarter-deceleration (QD)
V. Mid-deceleration (MD)
VI. End Systole (ES)

This study specifically focuses on the Peak systole (III) phase, which represents the maximum velocity through aortic valve. The inlet velocity this phase was set to 1.0 m/s where this value chosen to represent a simplified yet physiologically plausible condition. This selection is supported by Zolfaghri et al. [14] who identified it as a standard velocity waveform commonly used. Meanwhile, Table 2 tabulates the time velocity relations extracted from Fig. 2. The velocity is applied at the inlet boundary of the aorta valve. This study focuses on peak flow (III), which signifies the maximum velocity point at 1 m/s.

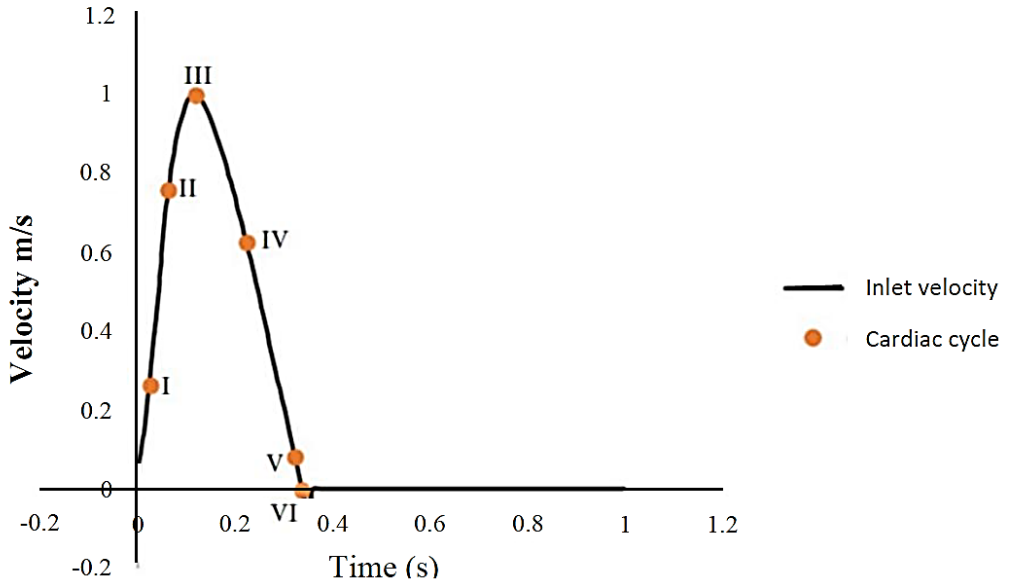

Fig. 2 *Velocity as a function of time, is applied at the inlet boundary. Six points of the heart presented: (I) Middle acceleration (MA), (II) three-quarters acceleration (3qa), (iii) peak flow (pf), (iv) quarter-deceleration (qd), (v) mid-deceleration (md) and (vi) end systole (es) [14]*

Int. Journal of Integrated Engineering Vol. 17 No. 4 (2025) p. 288-300

Table 2 *Indicator of the velocity profile used in this study*

	Cardiac Cycle	Time (s)	Velocity (m/s)
I	Middle acceleration (MA)	0.02	0.26
II	Three-quarters acceleration (3QA)	0.06	0.76
III	Peak flow (PF)	0.12	1.00
IV	Quarter-deceleration (QD)	0.22	0.62
V	Mid-deceleration (MD)	0.32	0.08
VI	End systole (ES)	0.34	0

2.3.2 Parameter Assumption

The Reynold number (Re) is a key parameter used to determine the nature of blood flow. When the Reynold number, $Re \leq 2000$ the flow is classified as a laminar flow, while when the Reynold number reached to $Re \geq 3000$ the flow is considered as a turbulent flow [29]. Based on the Reynold number of 5148.57, the flow is classified as a turbulent flow which exceeds more than 3000. In addition to Reynold number, blood density and viscosity are also important parameters assumption in this study. Table 3 summarizes the parameter assumptions used during Peak flow phase.

Table 3 *The parameter assumption during the peak flow phase, including Reynold number, blood density and viscosity*

Parameter assumption	Value
Reynold number	5148.57
Blood density	1060 kg/m^3
Viscosity	0.0035 Pa

2.3.3 Boundary Condition

Three boundary conditions were applied to the aortic root which are inlet, wall and outlet. These boundary selections play a crucial role in the aortic root region to preventing backflow of the blood. Fig. 3 illustrates the boundary conditions setup in the CFD simulation using Ansys.

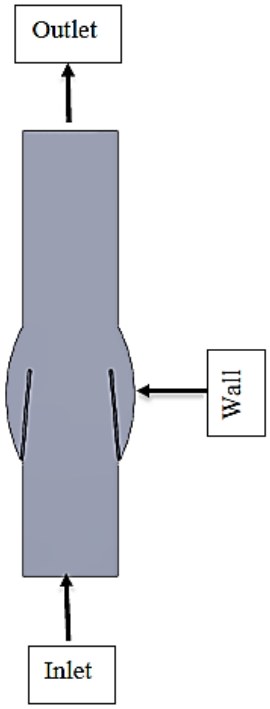

Fig. 3 *Boundary condition in aortic root*

2.4 Evaluation of Blood Flow Through the Aortic Valve

The velocities and pressure of the peak flow (PF) phase were computed in the simulation where assuming a steady-state flow condition at this phase. A condition involved the simulation to evaluate blood flow velocity before and after it passes through the valve at peak flow in a healthy state (Fig. 4 of 100% valve orifice model) and stenotic models (Fig. 5 of 50% valve orifice model). This setup was enabled to observe the blood flow velocity through the aortic root at the specific locations. The x-axis represents the distance along the aortic root. Line 1 (L1) is situated before the aortic valve, meanwhile Line 2 (L2) is positioned right after the valve. These lines are strategically placed to analyse the velocity patterns preceding and following the aortic valve. The range setup of velocity for each line varies. For L1 and L2, the velocity range is between 0 to 1.4 m/s, and between 0 to 16 m/s, respectively.

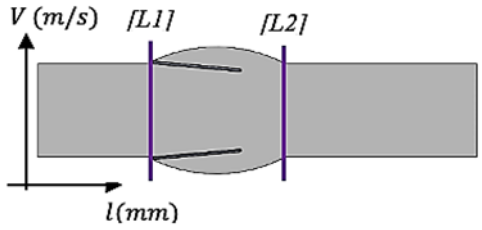

Fig. 4 *Lines 1 and 2 setups along the aortic root in 50% valve orifice model*

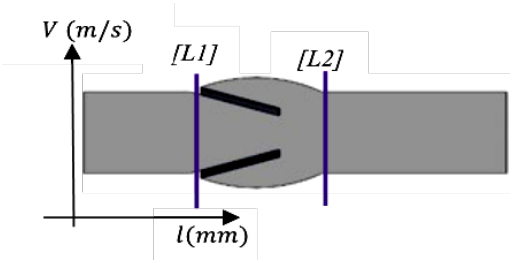

Fig. 5 *Lines 1 and 2 setups along the aortic root in 100% valve orifice model*

3. Results and Discussion

3.1 Visualization of the Blood Flow Velocity Streamline Characteristic

Fig. 6 illustrates a velocity streamline in the aorta, featuring both a healthy and a stenotic valve orifice, observed during peak flow. The range of the streamline velocity was set from 0 m/s to 5 m/s. The blue colour indicates regions of lower velocity, while the red colour represents regions of higher velocity. Two primary regions of vortex formation can be observed. First condition occurs after the narrowing of the valve which is at the wall of aortic root, meanwhile second condition occur at the aortic valve. 50% valve orifice shows more vortices occurs near wall compared to the 100% valve orifice model. In the stenotic model of 50% valve orifice, there were some turbulence and vortices occurring at the wall right after the valve region. Vortex and turbulence were caused by narrowing of the valve. As the valve narrows, the likelihood of a vortex forming and damaging the vessel increases. In a completely normal model, no vortex is produced due to the absence of narrowing in the healthy valve orifice.

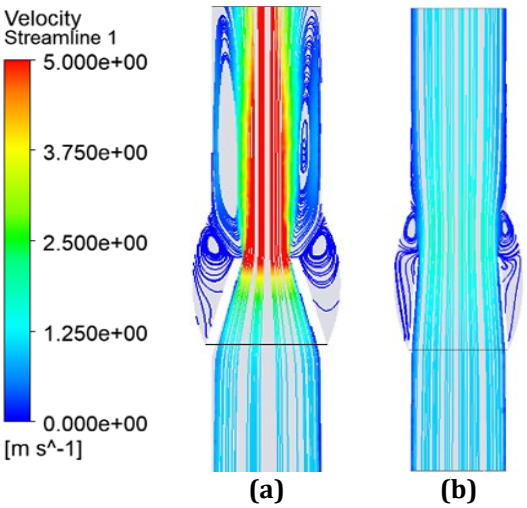

Fig. 6 *The visualization of streamline velocity magnitude along aortic root (a) 50% valve orifice model; (b) 100% valve orifice model*

In addition, the models with narrowing valve produce a vortex at the top of the valve due to the shape and dynamics of the valve leaflets and the force exerted by the blood flow. Vortex aids in reducing energy loss, constricting blood flow, and alleviating the heart's workload. Furthermore, vortices also prevent stagnation of

Int. Journal of Integrated Engineering Vol. 17 No. 4 (2025) p. 288-300

blood flow near the valve leaflets [30]. When stagnant blood flow occurred, plaque formation was potentially at risk. Consequently, the swirling motion of vortices assists in maintaining blood flow and preventing stagnation near the valve. Moreover, Nowak et al. [31] conducted a study using particle image Velocimetry (PIV) and found that vortex formation occurs at the top of the healthy aortic valve as shown at Table 4. The authors concluded that the vortex observed in the healthy valve demonstrated good agreement with the expected flow regime and resulted in the formation of circulating eddies. Similarly, the current simulation shows vortex formation at the top of the valve, aligning well with Nowak's finding. These vortices play beneficial role in preventing stagnant blood flow near the valve region.

Table 4 *Comparison of PIV and experiment from Nowak et al. [31] and simulation study*

	Vortices occur at the tip of the valve
PIV & Experiment [31]	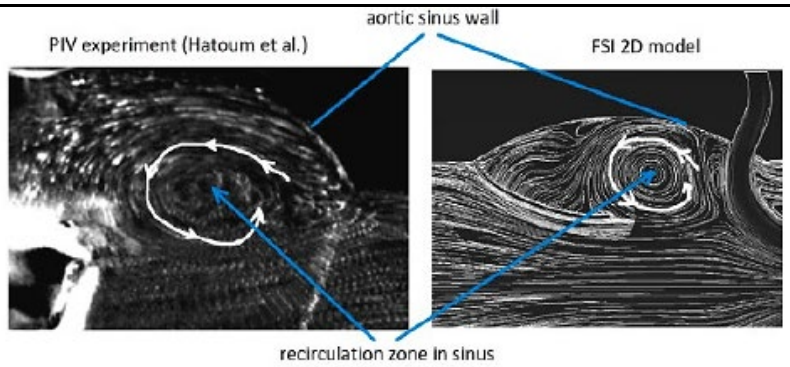
Study simulation	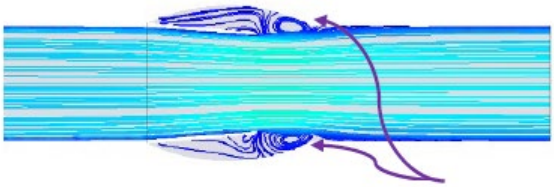

3.2 Visualization of the Blood Pressure Along the Aortic Root

Fig. 7 shows the blood pressure contour in unit Pascal (Pa), with blood pressure visualised along the aortic root in a stenotic 50% valve orifice and a healthy 100% valve orifice. During the peak flow phase, the stenotic model displayed elevated pressure ranging from 15 kPa to 9 kPa. This indicated increased pressure upon entering the aortic root inlet and decreased pressure in the post valve area, extending to the outlet of the aortic root. In contrast, the healthy 100% valve orifice model demonstrated lower pressure contours at the region near the outlet and inlet, which is between 0 kPa and 1.5 kPa. The lower pressure indicates that the healthy patient's heart valve does not have a stenosis problem.

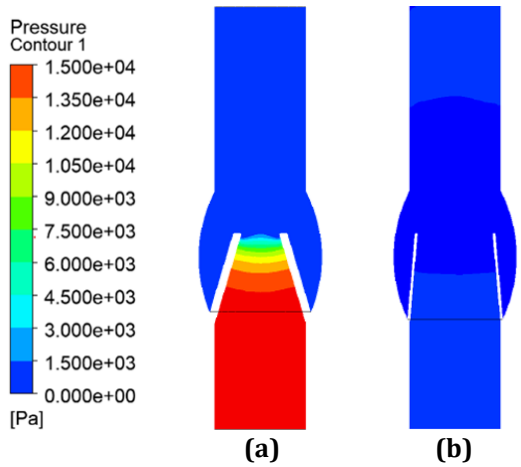

Fig. 7 *The visualisation of pressure contour along aortic root (a) 50% valve orifice model; (b) 100% valve orifice model*

3.3 Observation of Blood Flow Velocity in the Different Valve Orifice and Velocity

Fig. 8 shows the velocity profile during the peak flow along the aortic root, Y(m) for the two models. The highest velocity in the stenotic 50% valve orifice model is 0.61 m/s. Meanwhile, healthy 100% valve orifice models showed the lowest velocity at the maximum peak of 0.16 m/s. The maximum velocity value in both models is located at the opening of the valve region. Thus, the smaller the valve orifice, the higher the velocity occurred after the valve region.

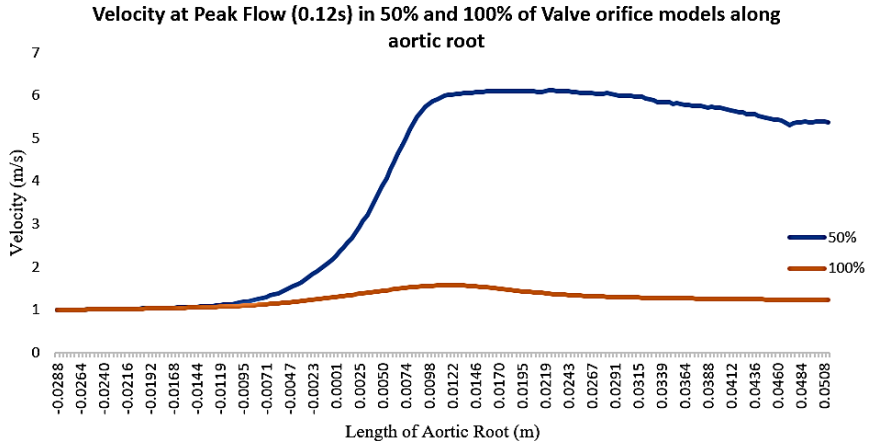

Fig. 8 *Velocity of two models along the aortic root (Blue: 50% Valve orifice; Orange: 100% valve orifice)*

Fig. 9 and Fig. 10 demonstrate the velocity profile at the peak flow during 0.12s, and the inlet velocity profile is 1.00 m/s. Peak flow is crucial for observing the velocities that occur at the aortic root. In Fig. 8 (a), the healthy 100% valve orifice model showed a maximum velocity of 1.10 m/s at L1 before the aortic valve region. Meanwhile, the stenotic 50% valve orifice recorded an increased maximum velocity of 1.21 m/s (Fig. 8 (b)). When the blood passed through the valve region, the stenotic aortic model showed a higher velocity profile during L2 at 6.09 m/s (Fig. 9 (b)) compared to the healthy one at 1.50 m/s (Fig. 9(a)). The model's velocity rise was attributed to the smaller valve orifice, which resulted in decreased pressure (Fig. 6 (b)) and a faster velocity streamline (Fig. 5 (b)).

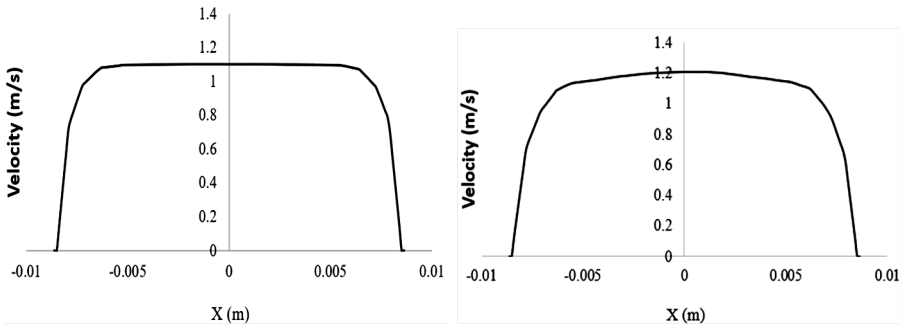

Fig. 9 *Line 1 (L1) velocity profile (a) Healthy 100% valve orifice; (b) Stenotic 50% valve orifice*

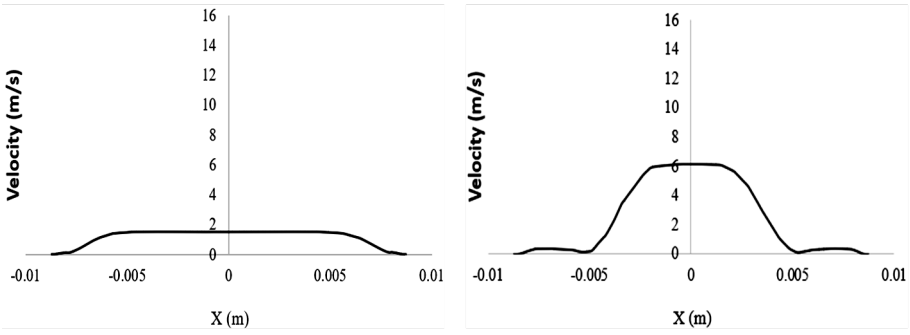

Fig. 10 *Line 2 (L2) velocity profile (a) Healthy 100% valve orifice; (b) Stenotic 50% valve orifice*

Int. Journal of Integrated Engineering Vol. 17 No. 4 (2025) p. 288-300

3.4 Evaluation Results on Critical Parameters for TAWSS, OSI, and RRT

Table 5 presents statistical data of kurtosis (K), area-mean average (μ), standard deviation (SD), and skewness (S) for TAWSS, OSI and RRT. The kurtosis analysis of TAWSS showed that the stenotic 50% valve orifice exhibited a higher positive kurtosis value of 303.03, while the healthy 100% valve orifice had the lowest value at 7.6049. A higher kurtosis value indicates increased shear stress and turbulence due to higher velocity after the valve orifice. Paisal et al. [32] stated that highest value in statistical data of kurtosis at parameter TAWSS considered worse [32]. The increasing kurtosis at 50% orifice model shows a potentially indicated a flow recirculation or vortex near the wall and aortic valve that caused by narrowed valve opening. The area-mean average provided insights into the shear stress experienced by the narrowed valve, with the stenotic 50% valve orifice showing a slightly higher mean TAWSS of 2.6845 compared to the healthy one. This suggests a greater risk of endothelial injury and plaque progression. SD analysis revealed greater variability in shear stress in the stenotic 50% valve orifice (7.7820) compared to the healthy one (1.4654), indicating turbulent flow that could accelerate valve damage. Skewness analysis showed a higher skewness value of 15.339 for the stenotic 50% valve orifice, compared to 1.5976 in the healthy 100% valve orifice, suggesting that shear stress was more unevenly distributed in the stenotic valve, potentially leading to adverse vascular effects.

Table 5 *Statistical parameter on kurtosis, min value, standard deviation and skewness at the aortic valve for TAWSS, OSI and RRT*

Parameters	Kurtosis (K)	Area-mean average (μ)	Standard deviation (σ)	Skewness (S)
TAWSS				
Model 50%	303.03	2.6845	7.7820	15.339
Model 100%	7.6049	1.3471	1.4654	1.5976
OSI				
Model 50%	3.6293	0.092261	0.1260	1.3064
Model 100%	4.9674	0.078163	0.1239	1.7461
RRT				
Model 50%	1194.4	96.473	1024.9	30.172
Model 100%	4092.3	6216.4	105140	57.714

The statistical analysis of OSI revealed that the kurtosis value for the healthy 100% valve orifice was 4.9674, while the stenotic 50% valve orifice exhibited the lowest value at 3.6293. Furthermore, the rise in skewness indicates noteworthy alterations in the valve's distribution shape. The stenotic 50% valve orifice shows a skewness value of 1.3064, less than the healthy one's value of 1.7461, reflecting a slight change in distribution. The area mean average for OSI was higher in the stenotic 50% valve orifice at 0.092261. In contrast, the healthy 100% valve orifice had the lowest value at 0.078163, reflecting an overall increase in oscillatory shear stress experienced by the valve. An increase in OSI, which reflects flow disturbances, may contribute to endothelial dysfunction and promote plaque formation, potentially reducing valve orifice size. Furthermore, the standard deviation (SD) analysis showed an increasing pattern from the healthy to the stenotic aortic valve, with the stenotic one showing a value of 0.1260 compared to 0.1239 in the healthy 100% valve orifice. An increase in the SD of OSI from the healthy to the stenotic models indicates more variability in oscillatory shear stress across the valve surface, probably due to changes in flow dynamics, including turbulence and disturbed flow patterns typical of stenotic valves.

In addition to the statistical analysis of OSI, the hemodynamic parameter of RRT is also vital for assessing the severity of aortic valve stenosis, as it pertains to TAWSS and identifies the most severe stenotic model. RRT measures the duration that blood particles remain near the wall after passing through the valve, which can be influenced by low velocity regions or flow recirculation. The kurtosis value for the healthy 100% valve orifice was higher than that of the stenotic 50% valve orifice, with a value of 1194.4, suggesting a more pronounced peak in residence time distribution. This increase indicates flow recirculation or vortex formation near the valve and wall due to a narrowed valve opening. The area mean average further supports this, with the stenotic 50% valve orifice showing the lowest value at 96.473, implying a shorter particle residence time due to higher post valve velocities.

The Standard Deviation of RRT is an important statistical measure as it reflects the variability and spread of residence time values within the valve region. SD analysis revealed that the stenotic 50% valve orifice exhibited the lowest SD at 1024.9, while the healthy 100% valve orifice had the highest at 105140, reflecting greater variability in particle residence time. The healthy valve showed a higher RRT SD which reflecting more variation in particle residence time due to recirculating flow zones. In contrast, the stenotic valve had a lower SD which indicating more uniform, jet-like flow that caused by the narrowed orifice. Additionally, skewness analysis revealed that the stenotic 50% valve orifice had a skewness value of 30.172, lower than the 57.714 observed in

the healthy one. Higher skewness is related to flow disturbances, recirculation zones, or vortex formation near narrowed valve openings.

4. Conclusions

Velocity analysis plays a key role in comprehending the hemodynamics of the aortic valve, especially during systole, offering essential insights for the progression and management of aortic stenosis (AS). Recent studies emphasise the significance of velocity analysis in evaluating the severity of AS and its effects on patient outcomes. For example, the echocardiographic evaluation of AS depends on peak velocity, mean pressure gradient, and aortic valve area (AVA) to gauge the hemodynamic impact of the effective orifice area and assess the severity of AS [6],[7] [33]. When blood flows past a blocked aortic valve, its velocity increases, converting static energy into kinetic energy and causing a pressure drop. As blood flow continues beyond the obstructed valve into the aorta, some kinetic energy is converted back into static energy, leading to a pressure recovery in the ascending aorta [7],[33]. CFD simulation software can also provide a detailed and accurate analysis of blood flow patterns in the aortic valve, which could help better understand the pathophysiology of AS and develop personalised treatment strategies [14]. By providing valuable insights into the hemodynamics of the aortic valve, velocity analysis can contribute to the development of innovative diagnostic and treatment strategies for AS [7],[14],[33], [34]. By using the statistical analysis, it provides a quantitative indicator that can support non-invasive diagnosis (simulation), risk prediction and treatment planning in patients with aortic valve stenosis. This study shows that the stenotic 50% valve orifice model showed a great difference in flow behaviour compared to a healthy one. This can be observed based on the velocity, pressure, streamline, TAWSS, OSI, and RRT hemodynamic results. This simulation may indicate risk factors related to heart failure because the blood velocity profile of the stenosed model exceeds that of the healthy 100% valve orifice model. The healthy 100% valve orifice model exhibited a healthy valve, and normal velocity occurred during the systole phase.

Future work will focus on integrating patient-specific geometries such as three leaflets of the valve and inlet conditions as well as validating these results against Particle Image Velocimetry (PIV) data. By doing the validation experimental, the proposed CFD framework can develop towards a personalized diagnostic tool that can help physician to make early decision-making and treatment for valvular heart disease. Additionally, it also can give benefit to family members of patients with aortic valve stenosis better understand the hemodynamic effects of the condition.

5. Limitations of the Study

A significant limitation of this study is the assumption of steady-state peak flow in the computational fluid dynamics (CFD) simulations. Aortic blood flow is inherently pulsatile and unsteady, characterized by rapid changes in velocity and pressure throughout the cardiac cycle However, the study assumed steady-state peak flow because the inlet velocity was fixed during the peak flow phase, therefore it exhibits stable hemodynamic characteristics over the specific duration, rendering the unsteady characteristics moot. Nevertheless, future studies should incorporate unsteady or pulsatile flow simulations to represent the dynamic and transient nature of aortic blood flow more accurately. Adding this parameter to the established time-dependent boundary conditions derived from patient-specific data, such as echocardiographic velocity profiles or pressure waveforms, would allow for a more comprehensive analysis of flow patterns, shear stress distribution, and pressure gradients throughout the entire cardiac cycle.

The second limitation is the absence of experimental validation. For the purpose of this study, even without immediate experimental validation, computational fluid dynamics (CFD) simulation results, particularly in the context of aortic stenosis, remain highly valuable and acceptable as a preliminary research step. This study's use of a stenotic 50% valve orifice model versus a healthy one serves as a crucial proof of concept and feasibility tool, demonstrating the ability of CFD to differentiate between healthy and diseased flow behaviors (velocity, pressure, streamlines, TAWSS, OSI, RRT) and predict a risk of heart failure due to elevated blood velocities in the stenosed model. Furthermore, these simulations contribute to understanding fundamental physics by clearly illustrating how blood flow past a blocked aortic valve increases velocity, converting static energy to kinetic energy and causing a pressure drop, followed by pressure recovery in the ascending aorta. This provides vital insights into the hemodynamic impact of the effective orifice area. Lastly, the ability to analyze detailed flow patterns allows for identifying critical parameters such as TAWSS, OSI, and RRT, which are crucial for evaluating AS severity and its effects on patient outcomes, thereby informing the development of innovative diagnostic and treatment strategies, even if subsequent unsteady simulations or experimental validation would provide a more complete picture.

Lastly, to address the limitation of the inlet velocity selection of 1 m/s for peak flow in this simulation, which appears low compared to physiological values (typically 4-6 m/s in stenotic conditions). However, this was a deliberate scaling approach to manage computational complexity and focus on the fundamental hemodynamic differences between healthy and stenosed valve models. By ensuring the Reynolds number (Re) remained within

a physiologically relevant turbulent regime (Re > 5000), the study could effectively capture key flow characteristics such as turbulence onset, jet formation, and pressure drop mechanisms. This approach allowed for a robust proof of concept, illustrating the distinct flow behaviors caused by the stenotic valve, and aided in understanding fundamental physics by clearly demonstrating the relative increase in velocity and pressure drop. It also helped identify critical parameters like TAWSS, OSI, and RRT, which indicate pathological conditions. Consequently, this steady-state, scaled simulation provides a valuable and computationally efficient foundation for understanding the relative hemodynamic impact of aortic valve stenosis, even as future research will incorporate more accurate, patient-specific pulsatile velocities for enhanced quantitative precision.

6. Data Availability Statement

The raw data supporting the conclusions of this article will be made available by authors, without undue reservation.

Acknowledgement

This research was supported by Universiti Tun Hussein Onn Malaysia through TIER1 (Vot Q542) and GPPS (Vot J043).

Conflict of Interest

Authors declare that there is no conflict of interests regarding the publication of the paper.

Author Contribution

The authors confirm contribution to the paper as follows: ***study conception and design****: Nur'Afifah Yousri, Ishkrizat Taib;* ***data collection****: Nabilah Ibrahim, Nur'Afifah Yousri, Ishkrizat Taib;* ***analysis and interpretation of results****: Nur'Afifah Yousri, Muhammad Riddha Abdul Rahman, Ali Kamil Kareem;* ***draft manuscript preparation****: Muhammad Riddha Abdul Rahman, Nur'Afifah Yousri. All authors reviewed the results and approved the final version of the manuscript*

References

[1] Ito Saki & Jae K. Oh (2022) Aortic stenosis: new insights in diagnosis, treatment, and prevention, *Korean Circulation Journal*, *52(10)*, 721-736. https://doi.org/10.4070/kcj.2022.0234

[2] Messika-Zeitoun David &Guy Lloyd (2018) Aortic valve stenosis: evaluation and management of patients with discordant grading, *E-Journal Cardiol Pract*, *15(26)*,

[3] Vavilis, Georgios, Magnus Bäck, Peter Bárány & Karolina Szummer (2022) Epidemiology of aortic stenosis/aortic valve replacement (from the Nationwide Swedish Renal registry), *The American Journal of Cardiology*, *163*, 58-64. https://doi.org/10.1016/j.amjcard.2021.09.046

[4] Pibarot Philippe & Marie-Annick Clavel (2022) Live longer and better without aortic valve stenosis, *The Lancet Healthy Longevity*, *3(9)*, e573-e574. https://doi.org/10.1016/S2666-7568(22)00188-X

[5] Sai Harika Pujari & Pradyumna Agasthi (2023 April 16). *Aortic Stenosis*. Treasure Island (FL): StatPearls Publishing. https://www.ncbi.nlm.nih.gov/books/NBK557628/

[6] Liam Ring, Benoy N. Shah, Sanjeev Bhattacharyya, Allan Harkness, Mark Belham, David Oxborough, Keith Pearce, Bushra S. Rana, Daniel X. Augustine, Shaun Robinson & Christophe Tribouilloy (2021) Echocardiographic assessment of aortic stenosis: a practical guideline from the British Society of Echocardiography." *Echo Research & Practice*, *8(1)*, G19-G59. https://doi.org/10.1530/ERP-20-0035

[7] Rachele, Manzo, Federica Ilardi, Dalila Nappa, Andrea Mariani, Domenico Angellotti, Maddalena Immobile Molaro & Giulia Sgherzi (2023) Echocardiographic evaluation of aortic stenosis: a comprehensive review, *Diagnostics*, *13(15)*, 2527. https://doi.org/10.3390/diagnostics13152527

[8] Zakikhani Parnia, Raymond Ho, William Wang & Zhiyong Li (2019) Biomechanical assessment of aortic valve stenosis: advantages and limitations, *Medicine in Novel Technology and Devices*, *2*, 100009. https://doi.org/10.1016/j.medntd.2019.100009

[9] Morris Paul D., Andrew Narracott, Hendrik von Tengg-Kobligk, Daniel Alejandro Silva Soto, Sarah Hsiao, Angela Lungu & Paul Evans (2016) Computational fluid dynamics modelling in cardiovascular medicine, *Heart*, *102(1)*, 18-28. https://doi.org/10.1136/heartjnl-2015-308044

[10] Yevtushenko Pavlo, Leonid Goubergrits, Benedikt Franke, Titus Kuehne & Marie Schafstedde (2023) Modelling blood flow in patients with heart valve disease using deep learning: A computationally efficient method to expand diagnostic capabilities in clinical routine, *Frontiers in Cardiovascular Medicine*, *10*, 1136935. https://doi.org/10.3389/fcvm.2023.1136935

[11] Syed Faiz, Sahar Khan & Milan Toma (2023) Modeling dynamics of the cardiovascular system using fluid-structure interaction methods, *Biology 12(7)*, 1026. https://doi.org/10.3390/biology12071026

[12] Khodaei Seyedvahid, Alison Henstock, Reza Sadeghi, Stephanie Sellers, Philipp Blanke, Jonathon Leipsic, Ali Emadi & Zahra Keshavarz-Motamed (2021) Personalized intervention cardiology with transcatheter aortic valve replacement made possible with a non-invasive monitoring and diagnostic framework, *Scientific Reports*, *11(1)*, 10888. https://doi.org/10.1038/s41598-021-85500-2

[13] Duronio Francesco & Andrea Di Mascio (2023) Blood flow simulation of aneurysmatic and sane thoracic aorta using OpenFOAM CFD software, *Fluids*, *8(10)*, 272. https://doi.org/10.3390/fluids8100272

[14] Zolfaghari Hadi, Mervyn Andiapen, Andreas Baumbach, Anthony Mathur & Rich R. Kerswell (2023) Wall shear stress and pressure patterns in aortic stenosis patients with and without aortic dilation captured by high-performance image-based computational fluid dynamics, *PLOS Computational Biology*, *19(10)*, e1011479. https://doi.org/10.1371/journal.pcbi.1011479

[15] Kamada Hiroki, Masanori Nakamura, Hideki Ota, Satoshi Higuchi & Kei Takase (2022) Blood flow analysis with computational fluid dynamics and 4D-flow MRI for vascular diseases, *Journal of Cardiology*, *80(5)*, 386-396. https://doi.org/10.1016/j.jjcc.2022.05.007

[16] Yong Lai Swee, Izuan Amin Ishak, Mohammad Arafat, Nurnida Elmira Othman, Nur Haziqah Shaharuddin & Nurshafinaz Mohd Maruai (2025) CFD Analysis on the Effects of Various Train Lengths on Aerodynamic Loads and Flow Structure for Train Travelling Through Various Crosswind Conditions." *Journal of Advanced Mechanical Engineering Applications* 6, no. 1 (2025): 70-79.

[17] Mahbubi, Muharis (2025) Comparative study of internal flow dynamics using CFD: T-junction pipe geometry, *Semarak Journal of Thermal Fluid Engineering*, *5(1)*, 11-20. https://doi.org/10.37934/sjotfe.5.1.1120a

[18] Mat Annur Adilia Maisarah (2025) A comparative study of internal flow dynamic using CFD: Simulation of turbulent flow in diffuser pipes, *Journal of Advances in Fluid, Heat, and Materials Engineering*, *5(1)*, 10-18. https://doi.org/10.37934/afhme.5.1.1018a

[19] Faro Abdulfatai, Kazeem Salam, Oludare Jeremiah, Isreal Akinwole & Animashaun Bukola (2021) Study of the stress distribution due to the effect of transient analysis on a vertical pressure vessel and validation using the mesh independence study, *Journal of Advanced Mechanical Engineering Applications*, *2(1)*, 1-12.

[20] Zbavitel Jan & Simona Fialová (2019) A numerical study of hemodynamic effects on the bileaflet mechanical heart valve, In *EPJ Web of Conferences*, 213, (pp. 02103). EDP Sciences. https://doi.org/10.1051/epjconf/201921302103

[21] Barua Saikat, Ishkrizat Taib, Nur'Afifah Yousri, Syafiq Suhaimi, Mian Sheng Wong, Wei Kang Wong & Mokhamad Fakhrul Ulum, Modelling analysis of face shield effectiveness against COVID-19 transmission, *Semarak Journal of Thermal Fluid Engineering*, *1(1)*, 11-22. https://doi.org/10.37934/sjotfe.1.1.1122a

[22] Fauzi Hilman, Achmad Rizal, Alvin Oktarianto & Ziani Said. "Classification of normal and abnormal heart sounds using empirical mode decomposition and first order statistic, *Journal of Electronics, Electromedical Engineering, and Medical Informatics*, *5(2)*, 82-88. https://doi.org/10.35882/jeeemi.v5i2.287

[23] Geeraert Patrick, Fatemehsadat Jamalidinan, Ali Fatehi Hassanabad, Alireza Sojoudi, Michael Bristow, Carmen Lydell, Paul WM Fedak, James A. White & Julio Garcia. "Bicuspid aortic valve disease is associated with abnormal wall shear stress, viscous energy loss, and pressure drop within the ascending thoracic aorta: a cross-sectional study, *Medicine*, *100(26)*, e26518. https://doi.org/10.1097/MD.0000000000026518

[24] DeCarlo Lawrence T (1997) On the meaning and use of kurtosis, *Psychological Methods*, *2(3)*, 292. https://doi.org/10.1037//1082-989X.2.3.292

[25] Kumar Pritam & Anurag Sharma (2024) Reynolds number effect on the parameters of turbulent flows over open channels, *AQUA—Water Infrastructure, Ecosystems and Society*, *73(5)*, 1030-1047. https://doi.org/10.2166/aqua.2024.056

[26] Shimoni, Sara, Iris Bar, Valery Meledin, Estela Derazne, Gera Gandelman, and Jacob George (2016) Circulating endothelial progenitor cells and clinical outcome in patients with aortic stenosis, *PLoS One*, *11(2)*, e0148766. https://doi.org/10.1371/journal.pone.0148766

[27] Barde, Mohini P & Prajakt J. Barde (2012) What to use to express the variability of data: Standard deviation or standard error of mean? *Perspectives in Clinical Research 3(3)*, 113-116. https://doi.org/10.4103/2229-3485.100662

[28] Yousri Nur'Afifah, Nabilah Ibrahim, Nur Amani Hanis Roseman, Ishkrizat Taib, and Shahnoor Shanta (2024) CFD based on the visualisation of aortic valve mechanism in aortic valve stenosis for risk prediction at the peak velocity." *Journal of Advanced Research in Micro and Nano Engineering*, *17(1)*, 56-68. https://doi.org/10.37934/armne.17.1.5668

[29] Zhu Yulei, Rui Chen, Yu-Hsiang Juan, He Li, Jingjing Wang, Zhuliang Yu, and Hui Liu (2018) Clinical validation and assessment of aortic hemodynamics using computational fluid dynamics simulations from computed tomography angiography, *Biomedical Engineering Online*, *17(1)*, 53. https://doi.org/10.1186/s12938-018-0485-5

[30] Gopal Arul Nalmanan Raja (2025) Comparative study of internal flow dynamics using CFD for of sudden expansion pipe, *Journal of Advances in Fluid, Heat, and Materials Engineering*, *5(1)*, 37-44. https://doi.org/10.37934/afhme.5.1.3744a

[31] Nowak Marcin, Eduardo Divo & Wojciech P. Adamczyk (2022) Fluid–structure interaction methods for the progressive anatomical and artificial aortic valve stenosis, *International Journal of Mechanical Sciences*, 227, 107410. https://doi.org/10.1016/j.ijmecsci.2022.107410

[32] Paisal Muhammad Sufyan Amir (2018) Computational analysis on stent geometries in carotid artery. [Doctoral dissertation, Universiti Tun Hussein Onn Malaysia].

[33] Geibel A., W. Kasper, G. Fraedrich, S. Konstantinides, J. Schöllhorn, N. Tiede & H. Just (1993) [Limitation of Doppler echocardiography in evaluation of aortic valve prostheses], *Zeitschrift fur Kardiologie*, 82(3), 175-180.

[34] Chenzbraun Adrian (2010) Pitfalls and challenges in the echocardiographic diagnosis of aortic stenosis, *European Cardiology Review*, *6(1)*, 10. https://doi.org/10.15420/ecr.2010.6.1.10

[35] Saiful Azam, S. R., Zainal Abidin, S. F., Ishak, I. A., Khalid, A., Mustaffa, N., Taib, I., Sukiman, S. L., & Darlis, N. (2023) "Flow analysis of intake manifold using computational fluid dynamics," *International Journal of Integrated Engineering*, vol. 15, no. 1, Apr. 2023. https://doi.org/10.30880/ijie.2023.15.01.008